ERJ Express. Published on July 9, 2008 as doi: 10.1183/09031936.00054608

PROPERTIES OF A STORE-OPERATED NON-SELECTIVE CATION CHANNEL IN AIRWAY SMOOTH MUSCLE

Peter B. Helli & Luke J. Janssen

Department of Medicine, McMaster University and the Firestone Institute for Respiratory Health, St. Joseph's Healthcare, Hamilton, Ontario, Canada

Running Head: BAPTA-evoked NSCC in ASM

Address correspondence to: Dr. Luke J. Janssen, St. Joseph's Hospital, room L314, 50 Charlton Avenue East, Hamilton, Ontario, Canada, L8N 4A6, Phone: (905) 522-1155, ext. 35912, Fax: (905) 540-6510, e-mail: janssenl@mcmaster.ca

Abstract

Passive depletion of internal Ca^{2+} stores in airway smooth muscle (ASM) activates non-selective cation channels (NSCCs) that mediate capacitative Ca^{2+} entry. However, the single channel properties of these cation channels have yet to be resolved and their regulation by cytosolic calcium levels ($[Ca^{2+}]_i$) still remains unclear. NSCC currents and changes in $[Ca^{2+}]_i$ during passive depletion of internal Ca^{2+} stores was monitored in isolated bovine tracheal myocytes. Loading cells with BAPTA-AM to reduce $[Ca^{2+}]_i$ and thereby deplete the store augmented a basal Gd^{3+}- and La^{3+}-sensitive, Ca^{2+}-permeable NSCC current. This current mimics that evoked by store depletion using the sarcoplasmic reticulum Ca^{2+} pump inhibitor cyclopiazonic acid (which concurrently and transiently elevates $[Ca^{2+}]_i$). Both interventions activated an ~25pS NSCC with properties identical to both spontaneous (basal) and BAPTA-evoked single channel currents. In summary, we provide novel evidence that a lanthanide-sensitive, 25pS NSCC underlies both basal and store depletion-evoked membrane currents in ASM and that this conductance likely contributes to the regulation of resting $[Ca^{2+}]_i$ and capacitative Ca^{2+} entry.

Key words: airway smooth muscle, BAPTA-AM, capacitative calcium entry, non-selective cation channel, single channel properties

Introduction

Agonist-mediated bronchoconstriction involves release of Ca^{2+} from the sarcoplasmic reticulum (SR) (1-4). The mechanisms responsible for store-refilling remain unclear, but seem to include voltage-gated Ca^{2+} channels (5), non-selective cation channels (NSCCs) (1;6;7) and/or reverse-mode Na^{+}/Ca^{2+} exchange (8;9). NSCCs formed by proteins of the transient receptor potential (TRP) family have received a great deal of attention, particularly those of the "canonical" or "classical" subtype (TRPC) (10-12).

In ASM, evidence of a functional link between TRPC expression and enhanced Ca^{2+}-influx (i.e. capacitative Ca^{2+}-entry, or CCE) remains sparse. Recently, White *et al*. demonstrated that disruption of endogenous TRPC3 expression in human ASM reduces both resting $[Ca^{2+}]_i$ and CCE (10): indirect pharmacological data suggest involvement of a NSCC, but membrane currents were not measured directly. Indeed, only a few studies have directly examined store depletion-evoked membrane currents in ASM (1;7;13). Hence it is not surprising that their single channel properties have yet to be resolved. In addition, many previous studies of CCE were done in the presence of agents which release stored Ca^{2+} (e.g., IP_3, caffeine) and/or which inhibit Ca^{2+}-reuptake by the SR Ca^{2+}-ATPase (SERCA) (e.g., cyclopiazonic acid, thapsigargin) (7;14-17). However, these approaches elevate $[Ca^{2+}]_i$ (4;14), which calls into question whether these currents are store depletion-activated or merely Ca^{2+}-dependent since ASM is known to express NSCCs that are facilitated by elevated $[Ca^{2+}]_i$ (2;6;18): in fact we found that the time course of activation of whole-cell NSCC currents by CPA in isolated bovine tracheal smooth muscle (TSM) cells paralleled the transient increase in $[Ca^{2+}]_i$ (7).

Therefore, to better understand the relationship between store depletion, activation of NSCCs and regulation of $[Ca^{2+}]_i$ in ASM, we compared activation of NSCC current during SR-

depletion by loading the cells with the Ca^{2+} chelator BAPTA versus inhibiting SERCA with CPA. We also probed the single channel properties of this conductance as well as the contribution of this and other Ca^{2+}-permeable channels in mediating Ca^{2+} entry upon SR Ca^{2+} depletion. Here, we report that depletion of SR Ca^{2+} stores in the presence or absence of cytosolic Ca^{2+} transients activates an ~25 pS NSCC which contributes to resting $[Ca^{2+}]_i$, CCE and likely functions to refill internal Ca^{2+} stores in ASM.

Materials and Methods

Tissues

All experimental procedures were approved by the McMaster University Animal Care Committee and conform to the guidelines set out by the Canadian Council on Animal Care.

Trachea from commercial cattle (136-454 kg) were obtained at a local abattoir and transported in ice-cold Krebs solution containing (in mM): 116 NaCl, 4.6 KCl, 2.5 $CaCl_2$, 1.3 NaH_2PO_4, 1.2 $MgSO_4$, 23 $NaHCO_3$, 11 dextrose and 0.01 indomethacin, bubbled with 95% O_2 / 5% CO_2 to maintain a pH of 7.4. ASM was dissected free of epithelium and connective tissue and maintained in Krebs solution at 4^{o}C for up to 48 hours.

Cell isolation

Bovine TSM strips were gently agitated for 20 minutes in modified Hanks balanced salt solution (with $NaHCO_3$, without $CaCl_2$ and $MgSO_4$) containing collagenase (Sigma blend type-F, 2 mg/ml) and elastase (type-IV, 250 μg/ml) at room temperature (21-23^{o}C), then for an additional 20-40 minutes at 37^{o}C. Cells were dispersed by gentle trituration with a wide-bore pipette, centrifuged, and re-suspended in standard Ringers solution containing (in mM): 130 NaCl, 5 KCl, 1 $CaCl_2$, 1 $MgCl_2$, 20 HEPES, 10 dextrose and 0.1 niflumic acid (omitted for Ca^{2+}-imaging); pH 7.4 with NaOH.

Electrophysiology

Single cells were allowed to adhere to the bottom of a recording chamber (1.5-ml volume) and then superfused with standard Ringers solution at room temperature (21-23^{o}C).

Electrophysiological responses were tested in cells that were phase-dense and appeared relaxed. Average cell capacitance was 59 ± 5 pF (*n*=13).

Whole cell currents were studied using the nystatin-perforated patch configuration of the standard patch-clamp technique. Pipettes with tip resistances of 3-5 MΩ were fashioned from borosilicate glass. Tip potentials were nulled and electrophysiological recordings commenced once series resistance dropped below 30 MΩ; 70-80% compensation was routinely employed. A holding potential of 0 mV was used to inactivate voltage-gated Ca^{2+} channels. Whole cell currents were low-pass filtered at 1 kHz, sampled and digitized at 2.5 kHz (DigiData 1200 A/D converter, Axon Instruments, Foster City, CA).

Liquid junction potentials (LJP) between the electrode and bathing solutions were 3.5 ± 0.3 (n = 6) and 11 ± 0.3 mV (n = 4) for standard Ringers and Na^+-free Ringers solution, respectively: reversal potentials (E_r) reported in the text were thus corrected as previously described (7), while current recordings shown in the figures were not.

Single channel currents from on-cell patches were filtered (5 kHz), sampled and digitized (20 kHz) using pipettes with tip resistances of 7-13 MΩ, and stored directly on a local hard-drive. Membrane potential was set to 0 mV by superfusing cells with a high molar KCl solution (see *Solutions and chemicals*). For off-line analysis and figure preparation, single channel currents were filtered at 500 Hz. To evaluate single channel current-voltage (I-V) characteristics, membrane potential was manually stepped from –120 to 60 mV. The transmembrane potential (V_m) is described by the equation $V_m = V_{cell} - V_{pipette}$; where V_{cell} is the membrane potential of the cell and $V_{pipette}$ is the potential imposed by the recording pipette. Assuming V_{cell} has been set to 0 mV by the external KCl solution, V_m is then the negative of

$V_{pipette}$. Inward channel currents are shown as downward deflections while outward currents are shown as upward deflections.

$[Ca^{2+}]_i$ fluorimetry

Single cells were incubated with fluo-4 AM (2 μM, containing 0.1% pluronic F-127) for 30 min at 37°C, then placed in a Plexiglas recording chamber and superfused with Ringers solution for 30 minutes to allow for dye de-esterification. Confocal microscopy was performed at room temperature (21-23^{o}C) as previously described (7). Video images (600x400 pixels; Video Savant 4.0; IO Industries, London, ON) were generated at 1 frame/sec for caffeine responses and 0.1 frame/sec for all other responses. Average fluorescence intensities from regions-of-interest (30x30 pixels) defined in central non-nuclear regions of cells were calculated for each frame and plotted against time. Relative changes in $[Ca^{2+}]_i$ were expressed in terms of a change in fluorescence (ΔF) over the initial/baseline fluorescence (F_o) observed in the presence of 1.8 mM extracellular Ca^{2+}. Caffeine was applied directly to cells via pipette driven by a pressure ejection system (Picospritzer^{TM} II, General Valve, Fairfield, NJ).

Solutions and chemicals

All drugs and reagents were obtained from Sigma Chemical Co. (Oakville, ON, Canada). Ca^{2+}-free Ringers contained (in mM): 130 NaCl, 5 KCl, 1 $MgCl_2$, 20 HEPES, 10 dextrose, 0.01 EGTA and 0.1 niflumic acid (omitted for Ca^{2+}-imaging); pH 7.4 with NaOH. Na^{+}-free Ringers solution consisted of (mM): 140 NMDG (N-methyl-D-glucamine), 5 KCl, 1 $CaCl_2$, 1 $MgCl_2$, 10 HEPES (pH 7.4 with NaOH), 10 dextrose and 0.1 niflumic acid; pH 7.4 with HCl. High molar

KCl Ringers solution contained (in mM): 126 KCl, 1.5 $CaCl_2$, 1 $MgCl_2$, 10 HEPES, 10 dextrose and 0.1 niflumic acid; pH 7.4 with NaOH

The intracellular electrode solution for measuring whole cell currents contained (mM): 130 CsCl, 5 $MgCl_2$, 1 $CaCl_2$, 10 HEPES and 5 EGTA; pH 7.2 with CsOH. These pharmacological and ionic conditions eliminated currents through Ca^{2+}-dependent Cl^- and K^+ channels. The standard electrode solution for on-cell recordings consisted of (mM): 126 NaCl, 1.5 $CaCl_2$, 10 HEPES and 10 dextrose; pH 7.4 with NaOH. For high-Ca^{2+} electrode solution, NaCl was replaced by 70 mM $CaCl_2$. All on-cell electrode solutions were supplemented with 10 mM tetraethylammonium chloride, 5 mM 4-aminopyridine, 100 μM niflumic acid and 1μM nifedipine to inhibit K^+-, Cl^-- and voltage-gated Ca^{2+} channels.

Nystatin for whole cell recordings was prepared in DMSO (30 mg/ml) for storage up to 5 days, and diluted to a final concentration of 300 μg/ml in electrode solution daily. Reagents were dissolved in aqueous media (Gd^{3+}, La^{3+}, caffeine), DMSO (CPA, BAPTA-AM, fluo-4 AM, nifedipine); the final concentration of DMSO in the bath was ≤ 0.001% in all cases.

Data analysis

Whole cell current records were obtained immediately before and during drug application, with each cell acting as its own control. In studies where channel inhibitors were used, data are reported as % inhibition of BAPTA-evoked current prior to subtraction of baseline current.

Unitary current amplitude histograms for individual patches were constructed from 0.5 to 2-sec sections of raw traces. I-V relationships, from individual patches in which unitary channel current amplitudes were measured at a minimum of three different membrane potentials, were

plotted and the unitary conductance and E_r for individual patches were then calculated using linear regression (least squares method). The mean unitary conductance and E_r were determined by averaging values from individual patches.

All data are reported as means ± SE, *n* values indicate number of animals tested; comparisons were made using a paired or unpaired Student's t-test or one-way ANOVA as appropriate, with *P* values < 0.05 considered significant.

Results

Differential effects of store depletion protocols on $[Ca^{2+}]_i$ and SR Ca^{2+} content

$[Ca^{2+}]_i$ responses evoked by a 10-s application of 10mM caffeine were utilized as an index of SR Ca^{2+} content. In the presence of 1.8 mM extracellular Ca^{2+}, repetitive caffeine stimulations at 5-min intervals evoked reproducible transient $[Ca^{2+}]_i$ elevations (Fig. 1A). In contrast, bathing cells in Ca^{2+}-free ringers for 10-min reduced baseline $[Ca^{2+}]_i$ ($\Delta F/F_o$=-15±3, n=35, P<0.001) and decreased the magnitude of caffeine-evoked transients by 52±13% (n=9, P=0.027), suggesting that basal Ca^{2+} entry is necessary for the maintenance of resting $[Ca^{2+}]_i$ and SR Ca^{2+} loading. L-type Ca^{2+} channels did not mediate this basal Ca^{2+} entry, since 1uM nifedipine did not significantly reduce baseline fluorescence ($\Delta F/F_o$=0.6±0.6, n=10, data not shown).

Both CPA and BAPTA-AM (10μM each) further reduced SR Ca^{2+} content such that caffeine-evoked $[Ca^{2+}]_i$ responses were reduced to a much greater extent than was seen following removal of extracellular Ca^{2+} alone (Fig. 1A). In the absence of extracellular Ca^{2+}, application of CPA evoked a transient rise in fluorescence, followed within 10-min by a sustained decrease to pre-drug levels (Fig. 1B); the rise in $[Ca^{2+}]_i$ likely reflecting Ca^{2+} leak from the SR via ryanodine receptors, while the return to baseline involves Ca^{2+} extrusion via the plasmalemmal Ca^{2+} pump ((4;5;14;19)). In contrast, treating cells with BAPTA-AM following removal of external Ca^{2+} caused a further decline in $[Ca^{2+}]_i$ that stabilized within 10-15-min (Fig. 1B).

Loading with BAPTA activates a NSCC in bovine TSM cells

In cells held under voltage-clamp, a small membrane current with mean amplitude of -82±19 pA at –60mV was observed. BAPTA-AM markedly increased the amplitude of this

current, which was stable for more than 30-min (Fig. 2). Voltage steps from –80 mV to +60 mV (10mV increments, 200 ms duration, from a holding potential of 0 mV) elicited currents that showed little time-dependent activation except at very negative potentials, and no deactivation over the 200 ms period of the voltage step (Fig. 2). The steady-state I-V relationship of both the baseline membrane current and BAPTA-evoked current were linear with E_r of +5.4±2.2 and -1.5±1.5 mV respectively (*n*=14) (Fig. 2). Instantaneous I-Vs obtained using ramp voltage commands (-100 to +80 mV, 2-sec duration, from a holding potential of 0 mV) were identical (*cf*. Fig. 3D).

Replacement of extracellular Na^+ with NMDG substantially reduced the inward portion of the BAPTA-dependent current (Fig. 3) such that the I-V relationship was now best described by a quadratic equation and E_r was displaced from -3.8±2.4 mV to -21±1.2 mV (*n*=4), representing a shift of -17 mV (95% CI of -13 to -21 mV, *n*=4) as would be expected if Na^+ were a major charge carrier for this conductance.

Next we examined the pharmacology of the BAPTA-activated current in these cells (results summarized in Table 1) by addition of blockers to the bathing medium. La^{3+}, which inhibits CCE in several ASM preparations (10;16;20), reduced BAPTA-evoked membrane currents but did not shift E_r (Fig. 4): this effect was concentration-dependent and poorly reversible. On the other hand, 10 μM Gd^{3+} (which has been widely utilized as an inhibitor of NSCCs and CCE in several smooth muscle cell types (21-23)) had little effect on the BAPTA-evoked current, although 100 μM caused a marked and irreversible suppression (Fig. 4).

Cell attached patches exhibit spontaneous single channel activity

To better understand the nature of the channel responsible for mediating resting and store-depletion evoked whole-cell membrane currents in bovine TSM cells, we examined single channel events recorded from cell-attached patches. Using high-K^+ Ringers to clamp V_m around 0 mV and a pipette solution containing 126 mM NaCl and 1.5 mM Ca^{2+}, we recorded discrete single channel openings at both positive and negative transmembrane potentials (Fig. 5A). In 8 of 18 cells examined, these spontaneous events were sufficiently frequent to allow for analysis of unitary current amplitudes: the I-V relationship of the spontaneous single channel currents had a slope-conductance of 26±0.3 pS with E_r=-2±3 mV (*n*=4; see Fig. 5B). When studied with a patch pipette containing 70 mM $CaCl_2$ the slope conductance was unchanged (24±2 pS) but the E_r was shifted leftward -14 mV (*P*=0.024, *n*=4; Fig. 5B), indicative of a high permeability to Na^+.

CPA and BAPTA-AM evoke single channel activity in previously quiescent patches

In membrane patches exhibiting little evidence of spontaneous single channel activity, treatment with 10 μM CPA or 10 μM BAPTA-AM substantially increased the number of single channel events (Fig. 6). The I-V relationships for these unitary events were linear in nature, with a slope-conductance of 23±1 and 26±1 pS and E_r occurring at -5±3 and -6±1 mV for CPA (*n*=7) and BAPTA-AM (*n*=3) respectively (126 mM NaCl electrode and 140 mM KCl bathing solution; see Fig. 6C). When studied with a 70 mM $CaCl_2$ pipette solution, the slope conductance and E_r of the CPA-evoked single channel current was 20±1 pS and -10±5 mV (*n*=3) respectively. The similarities in the properties of the spontaneous, CPA- and BAPTA-evoked single channel currents, as well as the similarity of their I-V relationship with that of the whole

cell current, suggests that the same NSCC underlies both spontaneous (baseline) as well as CPA- and BAPTA-evoked membrane currents.

Discussion

In many smooth muscle cell types, agonists release Ca^{2+} from an intracellular Ca^{2+} store (6;16;23). Subsequent restoration of cytosolic [Ca^{2+}] includes both re-uptake into the store by SERCA as well as extrusion from the cell by the plasmalemmal Ca^{2+}-pump and/or Na^{+}/Ca^{2+} exchanger. As such, there must be mechanisms in place to compensate for the net loss of cellular Ca^{2+} in order to avoid complete depletion of the store. In ASM, it appears that CCE, mediated by NSCCs, may be involved (1;5;7;13); however there are many unresolved issues regarding the electrophysiological properties, regulation and physiological roles of these channels. Notably, we present novel data regarding the single channel characteristics of this conductance. In the present study, we examined the properties of a membrane conductance activated by store depletion through either chelation of intracellular Ca^{2+} with BAPTA or inhibition of SERCA with CPA. In addition, we also examined the relative contribution of this channel in regulating $[Ca^{2+}]_i$ and CCE, with the goal of generating a better understanding of the ionic mechanisms underlying CCE in ASM.

Many of our isolated bovine TSM cells displayed NSCC currents at rest (*i.e.*, prior to store depletion); we have described this previously (7). NSCCs in ASM, whether activated by G-protein coupled receptor stimulation (6) or by passive depletion of SR Ca^{2+} (present study and (7)), are highly permeable to Na^{+}, conducting a significant inward Na^{+} current across a range of physiologically relevant membrane potentials (*e.g.* -60 to -30 mV). A large portion of the baseline and BAPTA-evoked NSCC currents in our study were also dependent upon extracellular Na^{+} (Fig. 3). These channels are also known to conduct Ca^{2+}. Although one estimate found this to comprise only 14% of the overall current, it is sufficient to maintain a modest yet sustained elevation of $[Ca^{2+}]_i$ (2;6). Others have demonstrated a constitutively active, nifedipine-

insensitive Ca^{2+} influx pathway in bovine TSM which they speculate contributes to a resting $[Ca^{2+}]_i$ around 100-150 nM (14;20). CPA enhances Ca^{2+} entry in several other ASM preparations presumably through activation of Ca^{2+}-permeable NSCCs (10;15;16;24). Basal NSCC currents have also been described in isolated smooth muscle cells from rabbit portal vein (25), ear artery (26) and coronary artery (22) as well as rat pulmonary artery (27).

The signaling pathway underlying activation of the store-operated NSCC currents is unclear. In the present study, G-protein coupled receptor signaling was not necessary for NSCC activation, since treatment with BAPTA or CPA alone was sufficient, although we cannot rule out the possibility that this current may be regulated through DAG- or PKC-dependent mechanisms as demonstrated in vascular smooth muscle (28). Also, although Ca^{2+}-dependent facilitation of NSCC currents has been described in equine (2;6) and porcine (18) TSM, we can rule out the possibility that this channel was merely regulated by Ca^{2+} or Ca^{2+}-dependent mechanisms, since CPA evokes a transient increase in $[Ca^{2+}]_i$ (7) whereas BAPTA suppresses $[Ca^{2+}]_i$.

In rabbit portal vein myocytes, spontaneous and store depletion-activated single channel events exhibit identical properties including unitary conductance, E_r and mean open times, suggesting that a similar channel underlies both currents (25). To determine if a similar mechanism operates in ASM, we conducted on-cell measurements of single channel currents both prior to and during passive store depletion with either CPA or BAPTA-AM. In all cell-attached patches examined, there was evidence of spontaneous single channel activity (~44% exhibiting robust activity), which we attributed to a NSCC given that conductance was permeable to Na^+ and Ca^{2+} and that membrane currents through Cl_{Ca}, K_V, K_{Ca} and VOC channels were eliminated by experimental design. Application of CPA or BAPTA-AM greatly increased

the frequency and number of unitary channel events observed: single channel analysis revealed this to be mediated by a unitary conductance of ~25 pS. The lanthanides Gd^{3+} and La^{3+} inhibit CPA-activated membrane currents and/or CCE in several tissues (16;21;27). In our study, application of 10 and 100 μM La^{3+} reversibly inhibited the BAPTA-evoked current in a dose-dependent manner. We also found this current to be largely resistant to 10 μM Gd^{3+}, although 100 μM Gd^{3+} caused a marked reduction of ~80%. In contrast to La^{3+}, the inhibitory effect required several minutes to develop fully and was irreversible. Others have similarly found that extracellular Gd^{3+} irreversibly blocks TRP3 currents in CHO cells with a late onset (29): the authors speculated that the kinetics of inhibition by Gd^{3+} in intact cells relies upon the uptake and extrusion rate of this cation, since the EC_{50} was lower and the rate of inhibition faster when Gd^{3+} was applied to the cytosolic face of the channel.

While others have shown that a 25 pS NSCC with similar properties (*i.e.*, unitary conductance and sensitivity to 1mM La^{3+}, Gd^{3+} and 100 μM SKF 96365) is activated by leukotrienes in isolated human BSM, its role in mediating CCE was not specifically examined (3). As such, our current finding that an ~25 pS channel underlies CPA- and BAPTA-evoked NSCC currents in bovine TSM is novel. The magnitude of the conductance described herein is ten-fold greater than that reported for store depletion-activated NSCCs in vascular smooth muscle cells (25;30;31): we cannot rule out the possibility that small conductance NSCCs were hidden within the noise inherent in our recordings. Involvement of this NSCC explains why the Ca^{2+} entry induced by CPA was resistant to nifedipine (Fig. 5). Bazan-Perkins and colleagues (2003) found the rate of Ca^{2+} entry in bovine TSM cells with depleted SR Ca^{2+} stores was resistant to D600 (20). Likewise in guinea pig TSM, depletion of SR Ca^{2+} with the SERCA inhibitor thapsigargin induces a rise in $[Ca^{2+}]_i$ and a contraction that is dependent upon $Ca^{2+}{}_o$, is

inhibited by Ni^{2+} and SKF 96365 but not nifedipine (15), and similar results have been observed in rat BSM upon depletion of ACh-sensitive stores (1).

In summary, we conclude that loading of bovine TSM cells with BAPTA (to reduce $[Ca^{2+}]_i$ and thereby deplete the store) augments a basal, Ca^{2+}-permeable non-selective cation conductance that is both Gd^{3+}- and La^{3+}-sensitive. In addition, our findings indicate that an ~25 pS NSCC underlies both basal, CPA- and BAPTA-evoked membrane currents in this tissue. Furthermore, our data suggest that NSCCs contribute to the regulation $[Ca^{2+}]_i$ and SR-refilling and are likely responsible for CCE observed in ASM.

Acknowledgements

These studies were supported by operating grants and Career Award (Luke J. Janssen) from the Canadian Institutes of Health Research (MOP 15561) and the Ontario Thoracic Society as well as a Student Fellowship Award (Peter B. Helli) from ALTANA Pharma.

References

1. Sweeney, M., McDaniel, S. S., Platoshyn, O., Zhang, S., Yu, Y., Lapp, B. R., Zhao, Y., Thistlethwaite, P. A., and Yuan, J. X. Role of Capacitative Ca2+ Entry in Bronchial Contraction and Remodeling. J.Appl.Physiol 2002;92(4):1594-602.

2. Wang, Y. X. and Kotlikoff, M. I. Signalling Pathway for Histamine Activation of Non-Selective Cation Channels in Equine Tracheal Myocytes. J.Physiol 15-2-2000;523 Pt 1:131-8.

3. Snetkov, V. A., Hapgood, K. J., McVicker, C. G., Lee, T. H., and Ward, J. P. Mechanisms of Leukotriene D4-Induced Constriction in Human Small Bronchioles. Br.J.Pharmacol. 2001;133(2):243-52.

4. Janssen, L. J., Wattie, J., Lu-Chao, H., and Tazzeo, T. Muscarinic Excitation-Contraction Coupling Mechanisms in Tracheal and Bronchial Smooth Muscles. J.Appl.Physiol 2001;91(3):1142-51.

5. Janssen, L. J. and Sims, S. M. Emptying and Refilling of Ca2+ Store in Tracheal Myocytes As Indicated by ACh-Evoked Currents and Contraction. Am.J.Physiol 1993;265(4 Pt 1):C877-C886.

6. Fleischmann, B. K., Wang, Y. X., and Kotlikoff, M. I. Muscarinic Activation and Calcium Permeation of Nonselective Cation Currents in Airway Myocytes. Am.J.Physiol 1997;272(1 Pt 1):C341-C349.

7. Helli, P. B., Pertens, E., and Janssen, L. J. Cyclopiazonic Acid Activates a Ca2+-Permeable, Nonselective Cation Conductance in Porcine and Bovine Tracheal Smooth Muscle. J.Appl.Physiol 2005;99(5):1759-68.

8. Hirota, S., Pertens, E., and Janssen, L. J. The Reverse Mode of the Na(+)/Ca(2+) Exchanger Provides a Source of Ca(2+) for Store Refilling Following Agonist-Induced Ca(2+) Mobilization. Am.J Physiol Lung Cell Mol.Physiol 2007;292(2):L438-L447.

9. Dai, J. M., Kuo, K. H., Leo, J. M., van Breemen, C., and Lee, C. H. Mechanism of ACh-Induced Asynchronous Calcium Waves and Tonic Contraction in Porcine Tracheal Muscle Bundle. Am.J Physiol Lung Cell Mol.Physiol 2006;290(3):L459-L469.

10. White, T. A., Xue, A., Chini, E. N., Thompson, M., Sieck, G. C., and Wylam, M. E. Role of TRPC3 in Tumor Necrosis Factor-Alpha Enhanced Calcium Influx in Human Airway Myocytes. Am.J.Respir.Cell Mol.Biol. 30-3-2006.

11. Freichel, M., Vennekens, R., Olausson, J., Stolz, S., Philipp, S. E., Weissgerber, P., and Flockerzi, V. Functional Role of TRPC Proteins in Native Systems: Implications From Knockout and Knock-Down Studies. J.Physiol 15-8-2005;567(Pt 1):59-66.

12. Albert, A. P., Pucovsky, V., Prestwich, S. A., and Large, W. A. TRPC3 Properties of a Native Constitutively Active Ca2+-Permeable Cation Channel in Rabbit Ear Artery Myocytes. J.Physiol 1-3-2006;571(Pt 2):361-9.

13. Peel, S. E., Liu, B., and Hall, I. P. A Key Role for STIM1 in Store Operated Calcium Channel Activation in Airway Smooth Muscle. Respir.Res. 2006;7:119.

14. Ethier, M. F., Yamaguchi, H., and Madison, J. M. Effects of Cyclopiazonic Acid on Cytosolic Calcium in Bovine Airway Smooth Muscle Cells. Am.J.Physiol Lung Cell Mol.Physiol 2001;281(1):L126-L133.

15. Ito, S., Kume, H., Yamaki, K., Katoh, H., Honjo, H., Kodama, I., and Hayashi, H. Regulation of Capacitative and Noncapacitative Receptor-Operated Ca2+ Entry by Rho-Kinase in Tracheal Smooth Muscle. Am.J.Respir.Cell Mol.Biol. 2002;26(4):491-8.

16. Ay, B., Prakash, Y. S., Pabelick, C. M., and Sieck, G. C. Store-Operated Ca2+ Entry in Porcine Airway Smooth Muscle. Am.J.Physiol Lung Cell Mol.Physiol 2004;286(5):L909-L917.

17. Pabelick, C. M., Ay, B., Prakash, Y. S., and Sieck, G. C. Effects of Volatile Anesthetics on Store-Operated Ca(2+) Influx in Airway Smooth Muscle. Anesthesiology 2004;101(2):373-80.

18. Yamashita, T. and Kokubun, S. Nonselective Cationic Currents Activated by Acetylcholine in Swine Tracheal Smooth Muscle Cells. Can.J.Physiol Pharmacol. 1999;77(10):796-805.

19. Tazzeo, T., Zhang, Y., Keshavjee, S., and Janssen, L. J. RYANODINE RECEPTORS DECANT INTERNAL Ca2+ STORE IN HUMAN AND BOVINE AIRWAY SMOOTH MUSCLE. Eur.Respir.J 19-3-2008.

20. Bazan-Perkins, B., Flores-Soto, E., Barajas-Lopez, C., and Montano, L. M. Role of Sarcoplasmic Reticulum Ca2+ Content in Ca2+ Entry of Bovine Airway Smooth Muscle Cells. Naunyn Schmiedebergs Arch.Pharmacol. 2003;368(4):277-83.

21. Flemming, R., Xu, S. Z., and Beech, D. J. Pharmacological Profile of Store-Operated Channels in Cerebral Arteriolar Smooth Muscle Cells. British Journal of Pharmacology 5-7-2003;139(5):955.

22. Terasawa, K., Nakajima, T., Iida, H., Iwasawa, K., Oonuma, H., Jo, T., Morita, T., Nakamura, F., Fujimori, Y., Toyo-oka, T., and Nagai, R. Nonselective Cation Currents Regulate Membrane Potential of Rabbit Coronary Arterial Cell: Modulation by Lysophosphatidylcholine. Circulation 10-12-2002;106(24):3111-9.

23. Wilson, S. M., Mason, H. S., Smith, G. D., Nicholson, N., Johnston, L., Janiak, R., and Hume, J. R. Comparative Capacitative Calcium Entry Mechanisms in Canine

Pulmonary and Renal Arterial Smooth Muscle Cells. J.Physiol 15-9-2002;543(Pt 3):917-31.

24. Ay, B., Iyanoye, A., Sieck, G. C., Prakash, Y. S., and Pabelick, C. M. Cyclic Nucleotide Regulation of Store-Operated Ca2+ Influx in Airway Smooth Muscle. Am.J.Physiol Lung Cell Mol.Physiol 2006;290(2):L278-L283.

25. Albert, A. P. and Large, W. A. A Ca2+-Permeable Non-Selective Cation Channel Activated by Depletion of Internal Ca2+ Stores in Single Rabbit Portal Vein Myocytes. J.Physiol 1-2-2002;538(Pt 3):717-28.

26. Albert, A. P., Piper, A. S., and Large, W. A. Properties of a Constitutively Active Ca2+-Permeable Non-Selective Cation Channel in Rabbit Ear Artery Myocytes. J.Physiol 15-5-2003;549(Pt 1):143-56.

27. Ng, L. C. and Gurney, A. M. Store-Operated Channels Mediate Ca(2+) Influx and Contraction in Rat Pulmonary Artery. Circ.Res. 9-11-2001;89(10):923-9.

28. Albert, A. P. and Large, W. A. Activation of Store-Operated Channels by Noradrenaline Via Protein Kinase C in Rabbit Portal Vein Myocytes. J.Physiol 1-10-2002;544(Pt 1):113-25.

29. Halaszovich, C. R., Zitt, C., Jungling, E., and Luckhoff, A. Inhibition of TRP3 Channels by Lanthanides. Block From the Cytosolic Side of the Plasma Membrane. J.Biol.Chem. 1-12-2000;275(48):37423-8.

30. Trepakova, E. S., Gericke, M., Hirakawa, Y., Weisbrod, R. M., Cohen, R. A., and Bolotina, V. M. Properties of a Native Cation Channel Activated by Ca2+ Store Depletion in Vascular Smooth Muscle Cells. J.Biol.Chem. 16-3-2001;276(11):7782-90.

31. Golovina, V. A., Platoshyn, O., Bailey, C. L., Wang, J., Limsuwan, A., Sweeney, M., Rubin, L. J., and Yuan, J. X. Upregulated TRP and Enhanced Capacitative Ca(2+) Entry in Human Pulmonary Artery Myocytes During Proliferation. Am.J.Physiol Heart Circ.Physiol 2001;280(2):H746-H755.

Figure Legends

Fig. 1. Effect of store depletion on $[Ca^{2+}]_i$ and SR Ca^{2+} content. A) Left: representative fluorimetric traces illustrating effects of removal of extracellular Ca^{2+} (*n*=9) - with or without concurrent treatment with 10 μM BAPTA-AM or 10 μM CPA - on $[Ca^{2+}]_i$ transients evoked by caffeine (10mM, 10 sec application; shaded squares). **Right:** mean data expressed both as $\Delta F/F_o$ (top) and as a ratio of the magnitude of the final caffeine response (C_{final}) relative to initial response ($C_{initial}$) (bottom) for control cells (*n*=10), zero-Ca^{2+} (*n*=9), zero-Ca^{2+} + BAPTA-AM (*n*=10), or zero-Ca^{2+} + CPA (*n*=8). *, $P < 0.05$ versus initial response in same group, paired, two-tailed, Student's t-test. $, $P < 0.05$, one-way ANOVA versus control. **B)** Left: representative traces illustrating changes in $[Ca^{2+}]_i$ following removal of extracellular Ca^{2+} followed by inhibition of SERCA with 10 μM CPA or passive loading with BAPTA (10 μM BAPTA-AM in bath). Right: mean change in $[Ca^{2+}]_i$ (*n*=12-35). *, significant change in $[Ca^{2+}]_i$ from baseline (F_o), $P < 0.05$, Student's t-test. #, $P < 0.05$ versus zero-$Ca^{2+}{}_o$, one-way ANOVA.

Figure 1

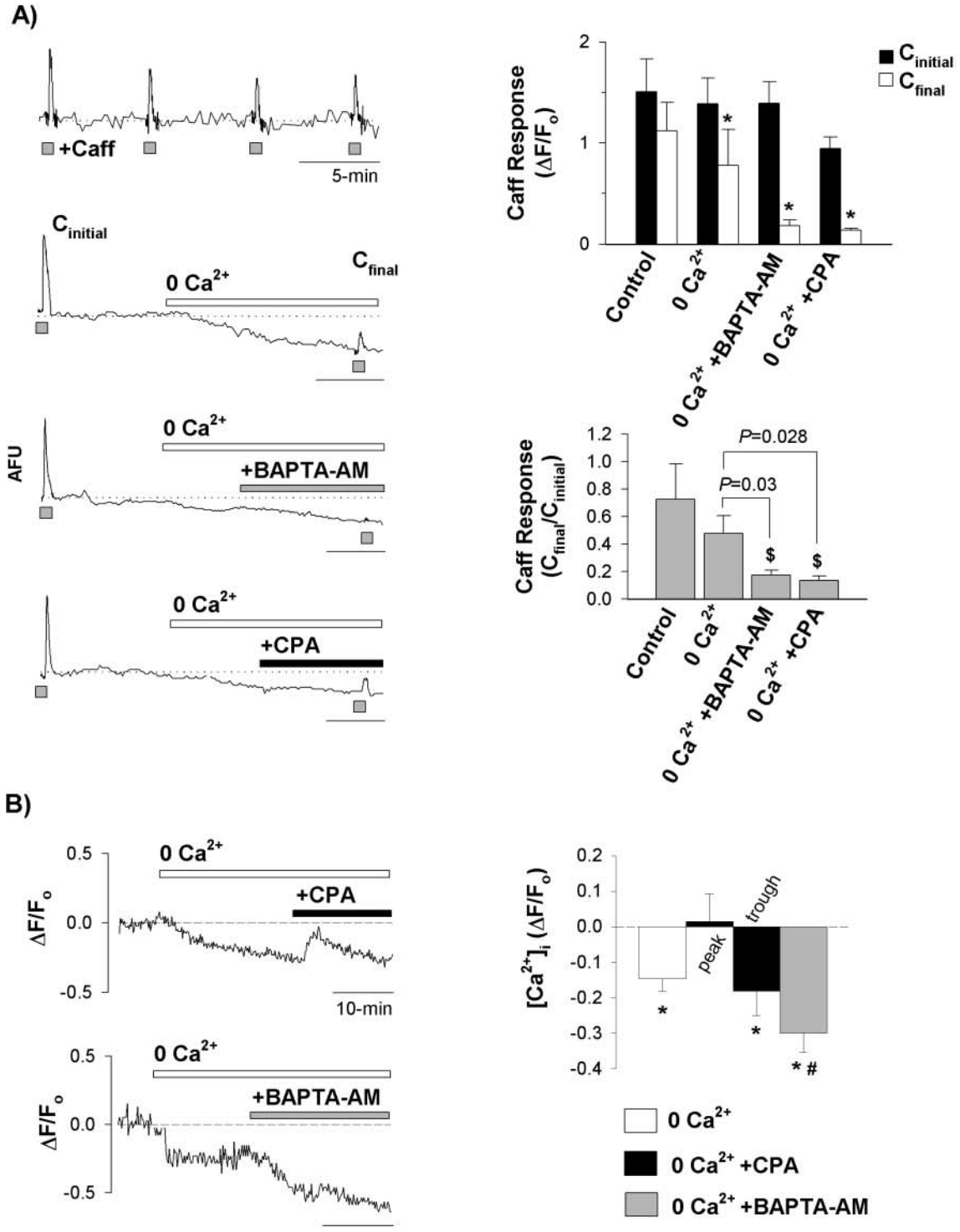
A)
+Caff
5-min
C initial
C final
0 Ca2+
AFU
+BAPTA-AM
+CPA
Caff Response (ΔF/Fo)
Control
0 Ca2+
0 Ca2+ +BAPTA-AM
0 Ca2+ +CPA
Caff Response (Cfinal/Cinitial)
P=0.028
P=0.03
$
B)
ΔF/Fo
10-min
[Ca2+]i (ΔF/Fo)
peak
trough
#

Fig. 2. Store depletion by BAPTA-AM augments a basal NSCC current. A) Representative traces of membrane currents evoked by voltage step pulses (200 ms duration; 10 mV increments) delivered from a holding potential of 0 mV before (left) and after (middle) application of 10μM BAPTA-AM; difference current given to right. **B)** Mean currents obtained prior to and during application of BAPTA-AM using voltage protocol in A (*n*=13).

Figure 2

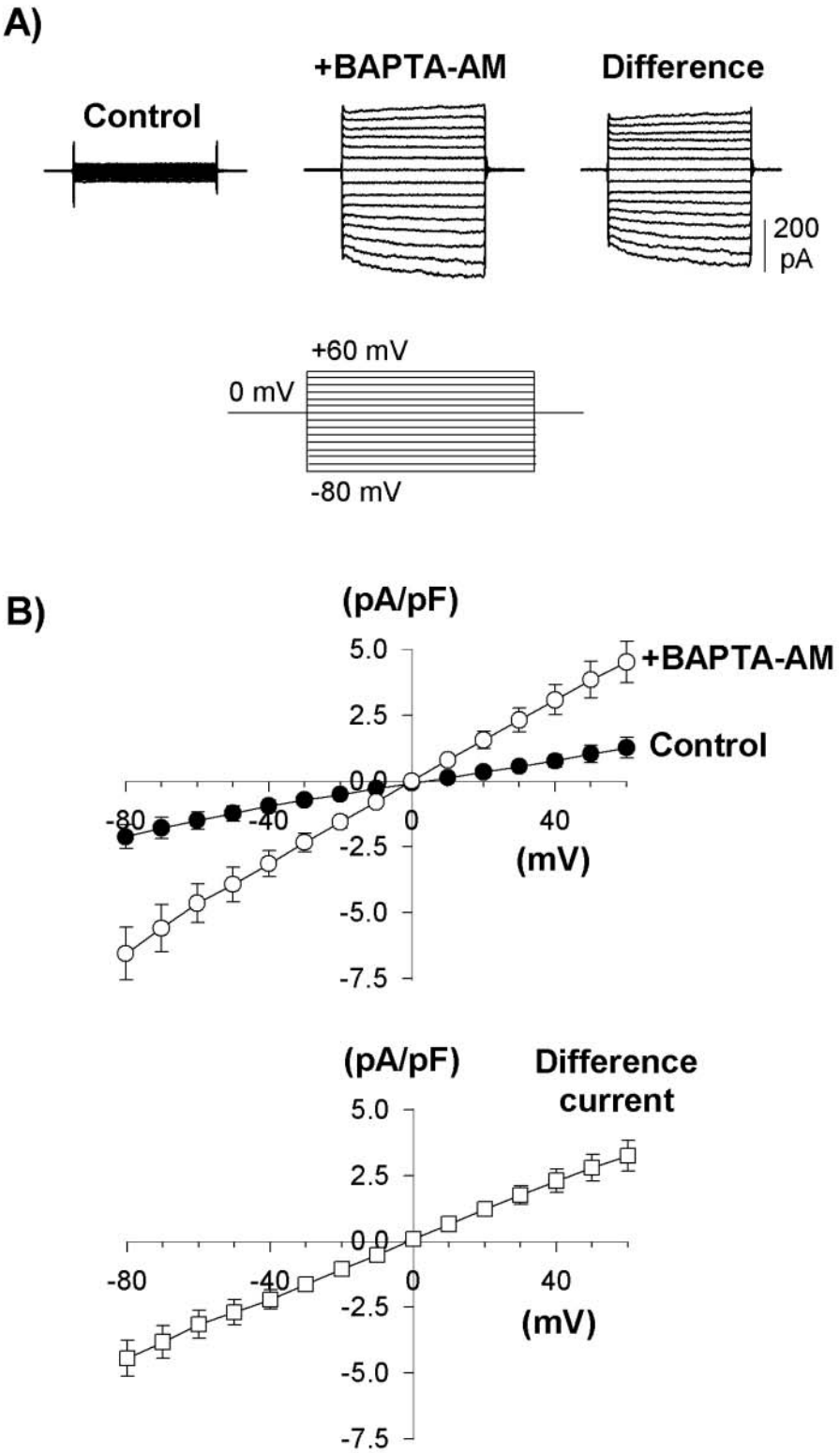
A)
Control
+BAPTA-AM
Difference
200
pA
+60 mV
0 mV
-80 mV
B)
(pA/pF)
5.0
2.5
0.0
-2.5
-5.0
-7.5
-80
-40
0
40
(mV)
+BAPTA-AM
Control
(pA/pF)
Difference
current
5.0
2.5
0.0
-2.5
-5.0
-7.5
-80
-40
0
40
(mV)

Fig. 3. Effect of removing external Na^+ on basal and BAPTA-evoked NSCC currents. A) Time course of BAPTA-evoked whole cell current. Filled circles represent mean current observed upon voltage stepping cell to -60 mV from a holding potential of 0 mV (200 ms duration, 10 sec intervals). Open horizontal bar denotes replacement of extracellular Na^+ in the bathing medium (flow rate of ~3 ml/min) with equimolar NMDG; gap in trace is 30-s. **B)** Current traces from cell in A at time-points indicated by Roman numerals. **C)** Mean basal (open bars, n=5) and BAPTA-evoked (solid bars, n=4) current at -60 mV before and after replacement of extracellular Na^+. **D)** Basal (control) and BAPTA-evoked (+BAPTA) membrane currents in the presence of Na^+ or following replacement with NMDG (-Na^+) obtained from a single cell studied using voltage ramps (right). #, $P < 0.05$, one-way ANOVA versus control. *, significant reduction upon removal of Na^+, $P < 0.05$, paired, two-tailed, Student's t-test.

Figure 3

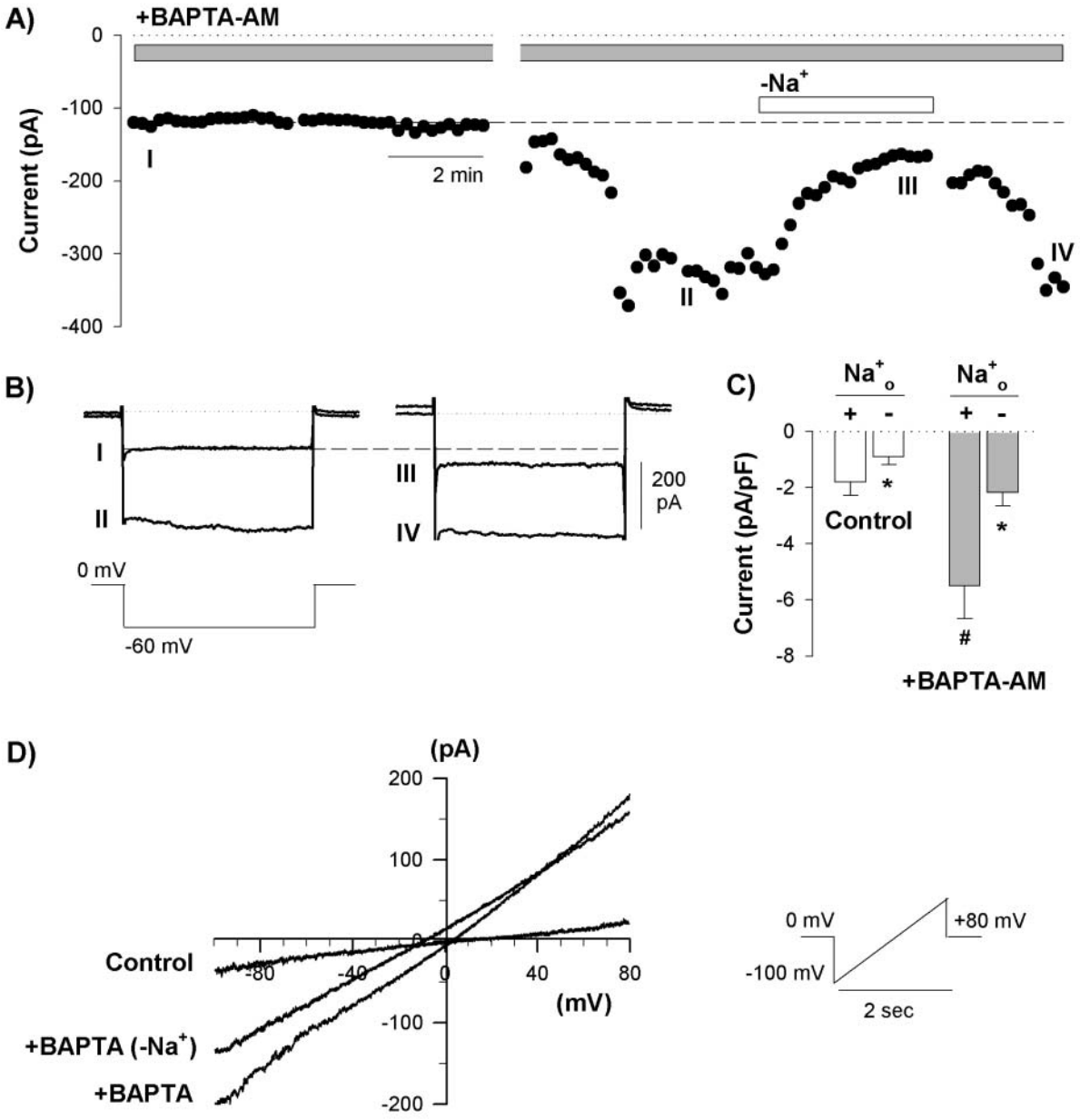

Fig. 4. Block of BAPTA-evoked whole cell current by La^{3+} and Gd^{3+}. A) Time course of inhibition of BAPTA-evoked membrane current by La^{3+} (top panel) or Gd^{3+} (bottom panel) in two separate cells. Filled circles represent the amplitude of inward membrane currents elicited by voltage stepping cells to -60 mV at 10-sec intervals. Breaks in graphs are 1 and 2-min respectively (omitted for clarity). **B)** Representative traces of membrane currents studied using voltage ramps in two separate cells. La^{3+} (left) and Gd^{3+} (right) were added to the bathing solution following activation of membrane current by 10 μM BAPTA-AM.

Figure 4

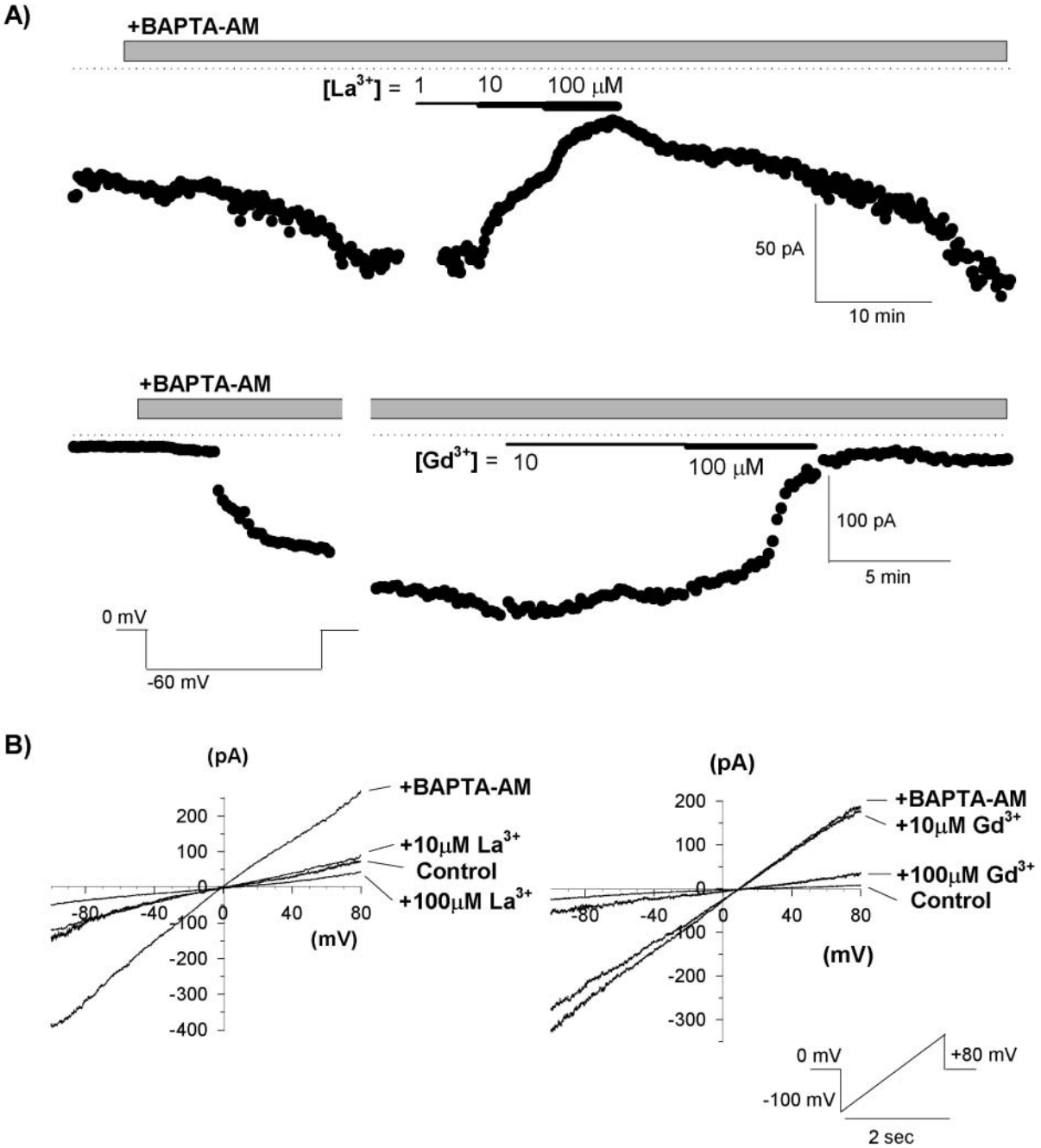

Fig. 5. Properties of spontaneous unitary NSCC events. A) Left: representative traces of spontaneous single channel currents observed in a cell-attached patch (126 mM $NaCl_2$ electrode). Solid line depicts closed channel state while dashed lines indicate predicted open states. Traces are 500 ms in duration. Right: all-points histograms for the traces shown at left. **B)** Mean I-V plots for spontaneous unitary channel currents studied with pipettes containing 126 mM $NaCl_2$ (filled symbols; $n = 4$) or 70 mM $CaCl_2$ (open symbols; $n = 4$).

Figure 5

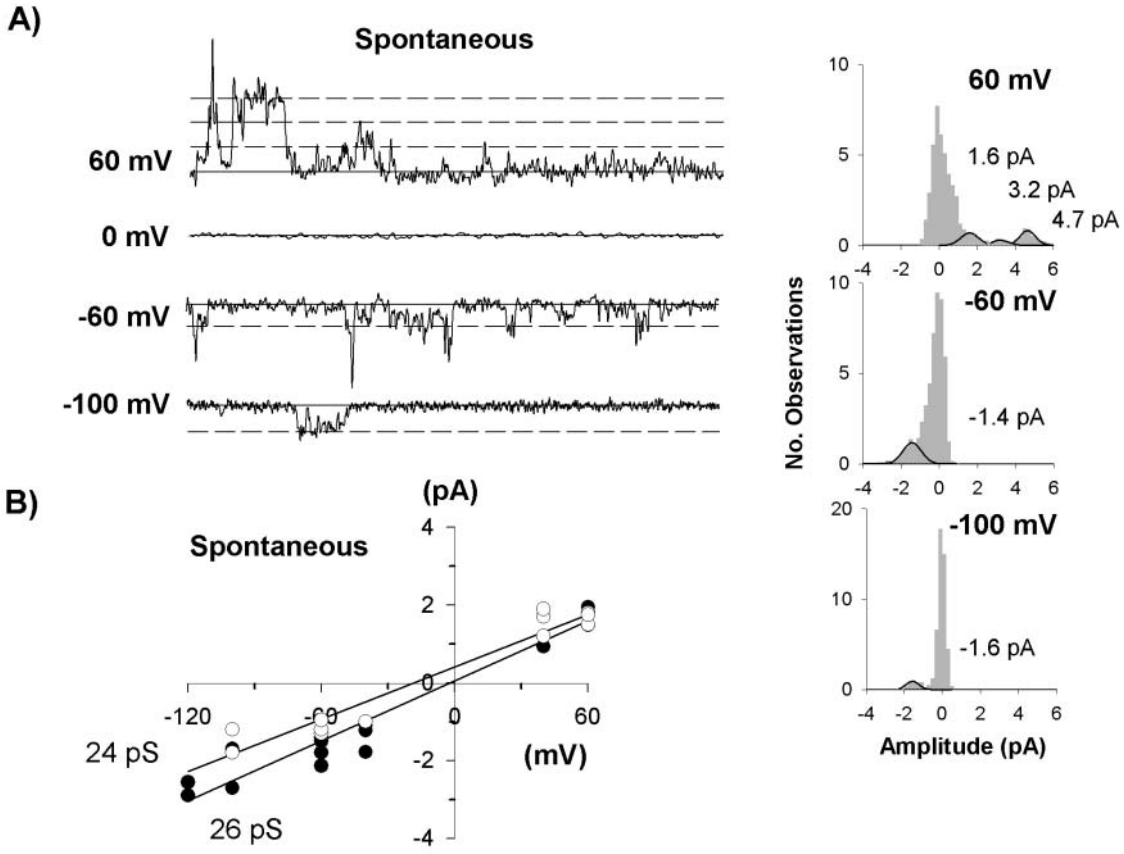

Fig. 6. Properties of CPA and BAPTA-AM-evoked single channel currents. Representative traces of single channel membrane currents induced by bath application of 10 μM CPA **(A)** or BAPTA-AM **(B)** at a transmembrane potential of -60 mV. 500 ms portions of recordings are expanded below: solid lines indicate closed channel state, while dashed lines depict predicted open channel states. Pipettes contained 70 mM $CaCl_2$ (A) and 126 mM NaCl (B). **C)** Mean I-V plots for CPA- and BAPTA-evoked unitary channel currents measured with pipettes containing 126 mM NaCl (filled symbols; $n = 7$ and 4 for CPA and BAPTA respective) or 70 mM $CaCl_2$ (open symbols; $n = 3$).

Figure 6

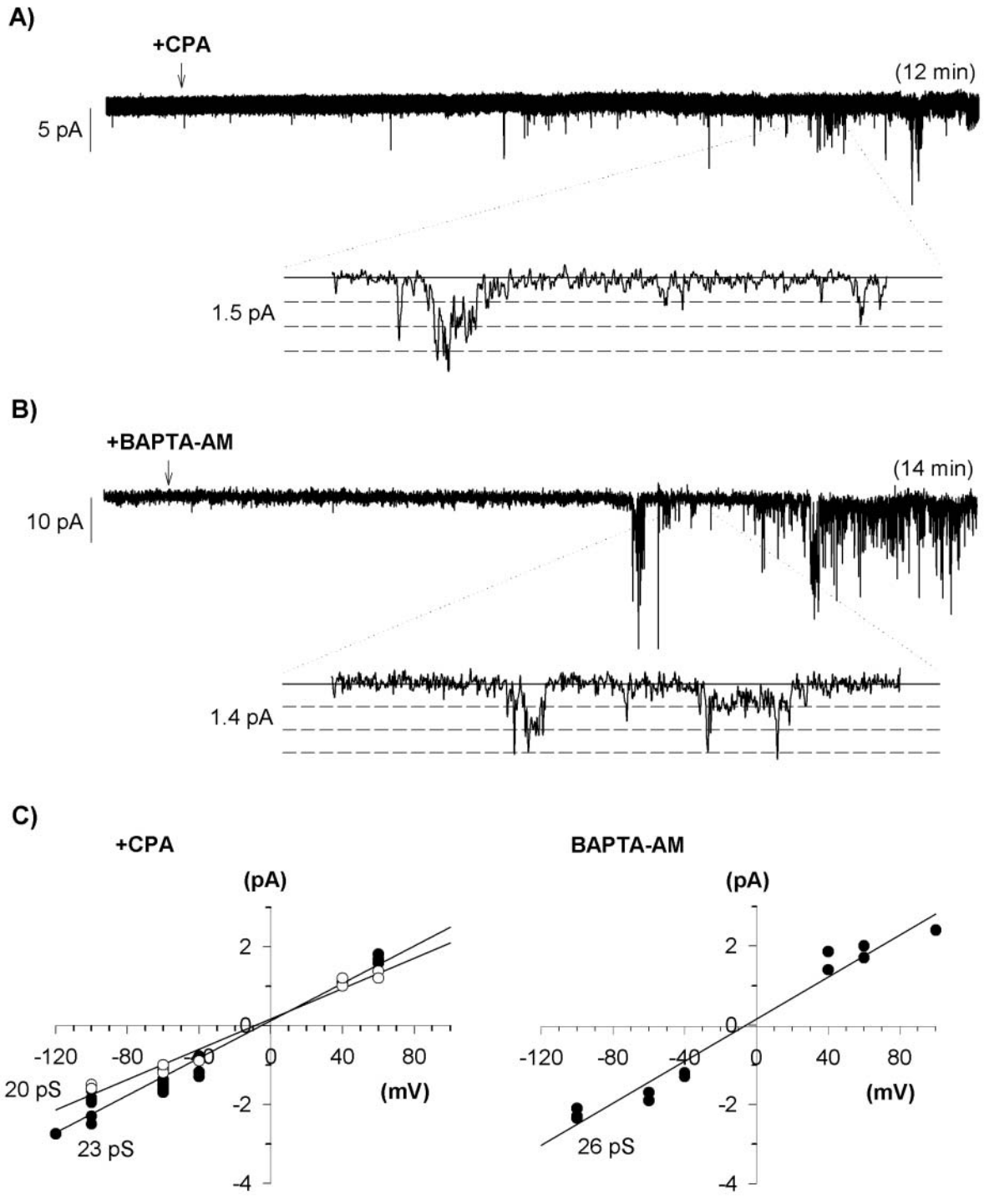
A)
+CPA
(12 min)
5 pA
1.5 pA
B)
+BAPTA-AM
(14 min)
10 pA
1.4 pA
C)
+CPA
BAPTA-AM
(pA)
(pA)
2
0
-2
-4
-120
-80
-40
0
40
80
(mV)
20 pS
23 pS
26 pS

Tables

Table 1. Pharmacological profile of BAPTA-AM-evoked membrane current in bovine tracheal smooth muscle cells measured at –60 mV.

Inhibitor	% inhibition BAPTA-AM-evoked current	*n* –value
10 μM Gd^{3+}	35 ± 15	6
100 μM Gd^{3+}	80 ± 5 *	6
1 μM La^{3+}	28 ± 15	4
10 μM La^{3+}	65 ± 8 *	5
100 μM La^{3+}	82 ± 3 *	5

Data are means ± SE. *$P < 0.05$, one-tailed, paired, Student's t-test.